Brucine-induced neurotoxicity by targeting caspase 3: Involvement of PPARγ/NF- κB/apoptosis signaling pathway

Yaying Lei
Zunyi Medical University
Fangqin Hou
Zunyi Medical University
Xiaoyu Wu
Zunyi Medical University
Yang Yi
Zunyi Medical University
Fan Xu
Albert-Ludwigs-University Freiburg
Qihai Gong
Zunyi Medical University
Jianmei Gao (gaojianmei@zmu.edu.cn)
Zunyi Medical University

Research Article

Keywords: brucine, neurotoxicity, transcriptome analysis, PPARγ, apoptosis, caspase 3

Posted Date: August 8th, 2022

DOI: https://doi.org/10.21203/rs.3.rs-1747852/v2

Abstract

Brucine, a weak alkaline indole alkaloid, is one of the main bioactive and toxic constituents of *Strychnos nux-vomica* L., which exerts multiple pharmacological activities, such as anti-tumor, anti-inflammatory, analgesic effect. However, its potential toxic effects limited its clinical application, especially central nervous system toxicity. The present study was designed to investigate the neurotoxicity and mechanism of brucine. Our results showed that brucine significantly induced Neuro-2a cells and primary astrocytes death, as evidenced by MTT assay and LDH release. Moreover, transcriptome analysis indicated that PPAR/NF-κB and apoptosis signaling pathways were involved in the brucine-induced cytotoxicity in Neuro-2a cells. Subsequently, in fact, brucine evidently inhibited PPARγ, promoted phosphorylation of NF-κB. Furthermore, PPARγ inhibitor aggravated the neurotoxicity, while, NF-κB inhibitor substantially reversed brucine-induced neurotoxicity. Moreover, brucine also significantly induced neuronal apoptosis and triggered increase in ratio of Bax/Bcl-2, level of cleaved caspase-3, as well as its activity as evidenced by TUNEL staining and Western blot. Furthermore, molecular docking analysis predicted that brucine directly bound to caspase 3. Intriguingly, a caspase 3 inhibitor (Z-DEVE-FMK) largely abolished the neurotoxicity of brucine. Our results reveal that brucine-induced neurotoxicity *via* activation of PPARγ/NF-κB/caspase 3-dependent apoptosis pathway. These findings will provide a novel strategy against brucine-induced neurotoxicity.

Introduction

Brucine is one of the major bioactive and toxic constituents of *Strychnos nux-vomica* L., which is a traditional Chinese medicine, and widely used for the treatment of rheumatic pain, cancers and so on (Savalia et al. 2017; Ma et al. 2018). While, clinical applications of brucine are limited due to its severe adverse drug effects, especially neurotoxicity (Li et al. 2018; Gao et al. 2021). Brucine-induced neurotoxicity mainly involves seizure, amyotrophy (Liu et al. 2015; Seeman et al. 2020). However, until now, the detailed mechanism of brucine-induced neurotoxicity remains still a mystery. Emerging evidence indicates that neuroinflammation and apoptosis play crucial roles in neurotoxicity (Zheng et al. 2013; Dang et al. 2021; Pei et al. 2021). Upon stimuli, neuroinflammation is evoked and coupled with the increased secretion of pro-inflammatory cytokines, which exacerbates neurotoxicity and results in irreversible neuronal apoptosis (Seshadri 2021; Hong et al. 2020). Apoptosis, one type of programmed cell death, is regulated principally by interactions within the B-cell lymphoma-2 (Bcl-2) family of proteins (Ney et al. 2021; Wang et al. 2020); among them, Bcl-2 and Bcl-2 associated X protein (Bax) are the vital members, which mediate multiple effectors thereby activating caspases (Reyna et al. 2017; Yang et al. 2020). Especially, activation of caspase 3, an eventual protein in the apoptotic cascade, leads to neuronal apoptosis (Chung et al. 2018; Huang et al. 2021). Of note, previous study revealed that brucine induces cancer cell apoptosis, along with decrease of Bcl-2, increase of Bax and caspase 3 (Seshadri 2021; Bahrami et al. 2017). Whereas, whether neuroinflammation and caspase 3-dependent apoptosis contribute to brucine-induced neurotoxicity remains unknown.

Thus, the present study was designed to unveil the potential mechanism of brucine-induced neurotoxicity. Transcriptomics, couple with molecular docking analysis indicated vital roles of neuroinflammation and apoptosis in brucine-induced neurotoxicity. Our results uncover that brucine induces neuronal apoptosis through mediating PPARγ/NF-κB/apoptosis signaling pathway. The findings highlight inhibition of caspase 3 or activation of PPARγ to hinder apoptosis as a potential strategy against brucine-induced neurotoxicity.

Materials And Methods

Chemicals and reagents

Brucine (purity ≥ 98% by HPLC) (Figure. 1A) was purchased from Nantong Feiyu Medical Biotechnology Corporation (Nantong, China). Brucine was dissolved in dimethyl sulfoxide (DMSO) at 10 mM as stock solution and the final concentration of DMSO in the media was less than 0.1%. 3-(4,5-dimethylthiazol-2-yl)-2,5- diphenyltetrazolium bromide (MTT, #M8180), Propidium Iodide (PI, #3843838) were from Sigma-Aldrich (St Louis, MO, USA). Fetal bovine serum (FBS, #1763585) and Dulbecco's modified Eagle's medium (DMEM, #8121436) were from Gibco BRL (Gaithersburg, MD, USA). Annexin V-fluorescein isothiocyanate (FITC, #556420) was obtained Becton Dickinson Pharmingen (Franklin Lake, New Jersey, USA). Mouse lactate dehydrogenase (LDH, #RJ17540), tumor necrosis factor alpha (TNF-α, #RJ17928), interleukin 1β (IL-1β, #RJ16944) and interleukin-6 (IL-6, #RJ16958) ELISA kits were from Shanghai Renjie Biotechnology (Shanghai, China). Caspase-3 Activity ELISA kit (#KD16967) was obtained from Guangzhou Kedi Biotechnology (Guangzhou, China). The antibodies against caspase 3 (#ab184787), cleaved caspase-3 (#ab214430), Bax (#ab182733), Bcl-2 (#ab59348), NF-κBp65 (#ab32536), phospho-NF-κBp65 (#ab76302), Peroxisome proliferation activating receptors (PPAR)α (#ab126235), PPARβ/δ (#ab178866), PPARγ (#ab209350) were from Abcam (Cambridge, UK).

Cell culture and drug treatment

The mouse neuroblastoma (Neuro-2a) cells were from American Type Culture Collection (Rockville, MD, USA) and were cultured with DMEM medium supplemented with 10% FBS and 1% penicillin/streptomycin. The cells were grown in a 5% CO_2 humidified atmosphere with 5% at 37°C. For brucine treatment, which was then appropriately diluted with serum-free DMEM before application. Neuro-2a cells were treated with different concentrations (1, 4, 16 μM) of brucine or co-treatment with 10 μM Z-DEVE-FMK (caspase 3 inhibitor), 10 μM GW 9662 (PPARγ inhibitor) or 20 μM Gliotoxin (NF-κB inhibitor) for 24 h.

Primary astrocytes were extracted from neonatal rat brains as our previous study (Zheng et al. 2020). The primary astrocytes were fixed with 4% paraformaldehyde, then incubated with anti-GFAP antibody, and visualized by an Alexa Fluor-conjugated secondary antibody. GFAP staining was used to identified the primary astrocytes up to more than 95% for the following experiment. Primary astrocytes were cultured with DMEM/F12 medium supplemented with 10% FBS and 1% penicillin/streptomycin. The cells were

grown in a 5% CO_2 humidified atmosphere with 5% at 37°C. Primary astrocytes were treated with different concentrations (8, 16, 32 μM) of brucine or 10 μM Z-DEVE-FMK (caspase 3 inhibitor) or 10 μM GW 9662 (PPARγ inhibitor) or Gliotoxin (NF-κB inhibitor) 24 h.

Cell viability determination

Neuro-2a cells (1×10^4) or primary astrocytes (1×10^4) were treated as mentioned above. At the end of treatment, 20 μl MTT (5 mg/ml) was added into the medium and cultured for another 4 h. Thereafter, the medium was carefully removed and 150 μl DMSO was added into each well. The optical density value of the cells was measured by a microplate reader at a wavelength of 490 nm. Cell viability was expressed as the percentage relative to the absorbance of the untreated control cells.

Detection of LDH level

The level of LDH of Neuro-2a or primary astrocytes after exposure of brucine was determined using a LDH assay kit. In brief, the Neuro-2a cells or primary astrocytes were treated as mentioned above. Briefly, supernatant was collected by centrifugation (3000 × *g*, 20 min), and the level LDH release was evaluated using a LDH assay kit according to the protocol's instructions. Thereafter, absorbance was detected at wavelength of 450 nm..

Cell morphological observation

For morphological observation, Neuro-2a cells or primary astrocytes were seeded in 6-well plates and treated with brucine as mentioned above. Then, the cells were observed by phase contrast microscopy (Olympus, IX53 + DP20, Japan).

Transcriptome analysis

Total RNA was extracted from the Neuro-2a cells of control and brucine group using TRIzol reagent according the experimental protocol, then quality of RNA samples quantified were detected based on Nanodrop ND-2000 system (Thermo Scientific, USA) and Agilent Bioanalyzer 4150 system (Agilent Technologies, CA, USA). Finally, qualified RNA transcriptome sequencing was performed with an Illumina Novaseq 6000 /MGISEQ-T7 instrument supported by Shanghai Applied Protein Technology. Principal component analysis (PCA), an unsupervised analysis that reduces the dimension of the data, was carried out to visualize the distribution and grouping of the samples, which was also commonly used to assess differences between groups and the quality of the biological replicates of samples within groups. Differential expression analysis was performed using the DESeq2 (http://bioconductor.org/packages/release/bioc/html/DESeq2.html), differential genes (DGEs) with |log2FC| >1 and adjusted p <0.05 were considered to be significantly different expressed genes. To directly observe the profile of potential DEGs, the up and down regulation of DEGs were visualized by volcano plot. Differential gene clustering is used to judge the changes of differential genes between brucine and control group. KEGG (Kyoto Encyclopedia of Genes and Genomes, http://www.kegg.jp/) is

one of the databases commonly used in pathway research. We use cluster Profiler R software package for GO function enrichment and KEGG pathway enrichment analysis, and $P < 0.05$, it is considered that the GO or KEGG function is significantly enrichment.

TUNEL staining

The apoptosis of Neuro-2a cells was detected using the TUNEL assay by the One Step TUNEL Apoptosis Assay Kit according to the manufacturer's instructions. Briefly, the Neuro-2a cells were treated as described above, then the cells were fixed with 4% paraformaldehyde for 30 min at room temperature, and then incubated with 0.3% Triton X-100 in PBS for 10 min. Thereafter, the Neuro-2a cells were incubated in TUNEL test solution at 37°C for 1 h in the dark; while, the cell nuclei were labeled using DAPI staining. And TUNEL-positive cells were observed using a fluorescence microscope (Olympus IX73, Olympus, Tokyo, Japan).

Detection of apoptosis using flow cytometry

The apoptosis of treated cells was examined using an Annexin V-FITC/PI apoptosis reagents according to the manufacturer's protocol. Briefly, the Neuro-2a cells were treated as mentioned above. The cells were then labeled with 500 μl binding buffer containing 2 μl Annexin V and 5 μl PI in the dark for 15 min after washed with PSB. Subsequently, apoptosis was detected using a flow cytometer (Navios, Beckman coulter, USA), and the Annexin V and PI values were set as the horizontal and vertical axes, respectively. Mechanically damaged, late apoptotic, dual negative/normal, and early apoptotic cells were located in the upper left, upper right, lower left and lower right quadrants of the flow cytometric dot plot, respectively.

Measurement of caspase 3 activity

The Neuro-2a cells or primary astrocytes were treated as described above. Cells supernatant was collected by centrifugation (3000 × *g*, 20 min, 4°C), and the caspase 3 assay was evaluated using caspase 3 assay kit according to the manufacturer's recommended protocol. Thereafter, absorbance was detected at wavelength of 450 nm, and all values of % caspase 3 activity were normalized to the untreated control group.

PPARγ activity assay

The primary astrocytes were treated as described above. The cells were dissolved in RIPI lysis buffer containing protease inhibitor and PMSF and kept on ice for 30 min. Then cells supernatant was collected by centrifugation (1000 *g*, 15 min, 4°C), protein concentration was determined by the BCA assay. The DNA-binding activity of PPARγ was evaluated by ELISA kit according to the manufacturer's recommended protocol. Thereafter, absorbance was detected at wavelength of 450 nm.

NF-κB DNA binding activity assay

Th primary astrocytes were treated with or without brucine as described above. Afterward, the NF-κB binding activity was following determined using the NF-κBp65 Transcription Factor Assay Kit according the manufacturer's instructions. Thereafter, absorbance was detected at wavelength of 450 nm.

Evaluation of inflammatory factors

The levels of inflammatory factors were detected using ELISA assay. Briefly, the Neuro-2a cells or primary astrocytes were treated as mentioned above. Then the supernatants were collected with centrifugation (3000 × *g* for 10 min at 4°C). Thereafter, the levels of IL-1β, IL-6 and TNF-α were detected according to the manufacturer's instructions.

Western blot analysis

RIPA buffer containing a protease and phosphatase inhibitor cocktail were added to the cells and homogenized at 4°C for 30 min. Then protein concentration was evaluated by BCA assay, and lysates were normalized to equal amounts of protein. Further, 10 μg proteins were separated by 12% or 10% sodium dodecyl sulfate-polyacrylamide gel electrophoresis and transferred onto a nitrocellulose membrane. Subsequently, the membranes were blocked with 5% fat-free dry milk at room temperature for 2 h. The blots were incubated with anti-caspase 3 (1:1000), anti-cleaved caspase 3 (1:1000), anti-Bcl-2 (1:1000), anti-Bax (1:1000), anti-NF-κBp65 (1:1000), anti-phospho-NF-κBp65 (1:1000), anti-PPARα (1:1000), anti- PPAR-β/δ (1:1000), anti-PPARγ (1:1000), anti-β-actin (1:5000) and GAPDH (1:5000) overnight at 4 °C. The membranes were washed with TBST and incubated with horseradish peroxidase-conjugated goat anti-rabbit IgG secondary antibodies (1:5000) at room temperature for 30 min. The proteins were finally examined using an enhanced chemiluminescence system and Image J microsoft was used to analyze the bands.

Molecular docking

Molecular docking analysis between brucine and caspase 3 were performed using Autodock 4.2 and Autodock Tools (ADT). In brief, the caspase 3 (Protein Data Bank ID:3KJF) protein were obtained from the Protein Data Bank database. A three-dimensional structure of brucine was established using the ChemBio3D Ultra 14.0 (PerkinElmer Informatics, USA), which was further proceeded using ADT. Thereafter, the molecular docking of the brucine and caspase 3 proteins was performed using Autodock 4.2.

Statistical analysis

All data were obtained from at least three independent experiments and ex-pressed as mean ± SD and were analyzed using SPSS version 18.0 (SPSS, Inc., Chicago, USA). Comparisons of the different groups were performed with Student's t-test. $P < 0.05$ was considered the minimal level of significance.

Results

Brucine induced cytotoxicity in Neuro-2a cells

In order to explore the effect of brucine on Neuro-2a cells, cell viability and cytotoxicity were evaluated by MTT method and LDH release, respectively. The results showed that brucine (1, 4, and 16 μM) significantly reduced cell viability in a concentration-dependent manner than that of control group (Figure 1B). In parallel, brucine markedly increased levels of LDH (Figure 1C). Moreover, after exposure to brucine, a reduced number and morphological changes in Neuro-2a cells were observed than that of control group (Figure 1D). These findings suggest that brucine exerted cytotoxicity on Neuro-2a cells.

Transcriptome processing and data analysis

PCA was commonly used to evaluate the differences between groups and the quality of the biological repetition of samples within groups. The PCA score plot showed that the gene expression between brucine treatment and control groups was significant (Figure 2A). Moreover, the volcano plot analysis showed that 727 DEGs were involved, among them, 186 genes were up-regulated and 541 genes were down-regulated (Figure 2B). The hierarchical clustering analysis of gene expression changes further revealed a clear separation between brucine and control group (Figure 2C). Furthermore, the results revealed that the top 20 pathways enriched from KEGG database, including NF-κB, PPARs and apoptosis signaling pathways (Figure 2D). These findings indcate that PPARγ/NF-κB/apoptosis sinaling pathway is involved in the brucine-induced cytotoxicity.

Brucine elicited inflammatory cytokines through regulating PPARγ/NF-κB signaling pathway

Based on the analysis of transcriptome, we further detected the levels of inflammatory cytokines and the protein expressions of PPARs and NF-κB by ELISA assay and Western blot, respectively. These results showed that the levels of IL-1β, IL-6 and TNF-α were remarkably increased after brucine treatment than those of control group (Figure 3A-C). Moreover, brucine significantly increased the phosphorylation level of NF-κBp65 than that of control group (Figure 3D, E). In addition, brucine evidently decreased the protein expression of PPARγ, but did not change the protein expressions of PPAR-α, PPAR-β/δ than those of control group (Figure 3F-I). These fingdings suggest that brucine promots inflammatory cytokine release through activating PPARγ/NF-κB signaling pathway.

Brucine induced cytotoxicity through inducing apoptosis

TUNEL staining was used to evaluate whether brucine-induced apoptosis in Neuro-2a cells. The results showed that brucine significantly increased the number of TUNEL-positive cells than that of control group (Figure 4A, B). Furthermore, the effect of brucine induced apoptosis in Neuro-2a cells were verified using Annexin V-FITC/PI staining by flow cytometry. The results demonstrated that apoptotic cells accounted for 6.5%, 38.7% and 54.3% after treatment with brucine (1, 4 and 16 μM) in a concentration-dependent manner (Figure 4C). These findings suggest that brucine-induced cytotoxicity through inducing apoptosis.

Brucine induced apoptosis through activation of caspase 3 pathway

Western blot was used to further explore the molecular mechanism of brucine-induced apoptosis. The results showed that brucine significantly increased Bax/Bcl-2 ratio and cleaved-caspase 3 level (Figure 5A-C), as well as caspase 3 activity than those of control group (Figure 5D). These findings indicate that brucine-induced cytotoxicity, at least partly, through caspase 3-dependent apoptosis pathway.

Brucine induced neurotoxicity on primary astrocytes

Based the findings mentioned above, we further investigate whether brucine-induced neurotoxicity. Since astrocyte is an important kind of neurocyte, which is rich of PPARγ and response to inflammation upon neurotoxic stimuli, we used primary astrocytes to determined the neurotoxic effect and its possible mechanism of brucine. The results showed that brucine (8, 16, 32 μM) remarkable reduced cell viability and increased LDH levels than those of control group in a dose-dependent manner (Figure 6A, B). Moreover, brucine (8, 16, 32 μM) also decreased the number of cells and led to the astrocytes collapse than that of control group (Figure 6C). These results suggest that brucine induced neurotoxicity.

Brucine increased the proinflammatory cytokines in primary astrocytes through PPARγ/NF-κB signaling pathway

To confirm the mechanism of brucine induced neurotoxicity, the levels of proinflammatory cytokines were measured by ELISA assay. The results showed that markedly brucine significantly increased the levels of IL-1β, IL-6 and TNF-α in primary astrocytes than those of control group (Figure 7A-C). Furthermore, the protein expressions of NF-κBp65 and PPARγ, as well as NF-κBp65 and PPARγ activities were evaluated using Western blot and appropriate activity kits, respectively. The results showed that brucine markedly increased phosphorylation level of NF-κBp65 and its DNA-binding activity in primary astrocytes than those of control group (Figure 7D-F). Additionally, brucine significantly decreased the protein expression of PPARγ and its DNA binging activity in primary astrocytes than those of control group (Figure 7G-I). These findings revealed that brucine-induced proinflammatory cytokines release is also through mediating PPARγ/NF-κB signaling pathway. To further investigate the mechanism by which brucine-induced neurotoxicity. We detected Bax/Bcl-2 ratio and caspase 3 activity. The results showed that brucine significantly increased Bax/Bcl-2 ratio (Figure 7J, K) and caspase 3 activity (Figure 7L) in primary astrocytes than those of control group. These findings demonstrate that brucine induced neurotoxicity through caspase 3-dependent signaling pathway.

Brucine-induced cytotoxicity and neurotoxicity through regulation of NF-κB/ PPARγ/caspase 3 pathway

The inhibitors of caspase 3, NF-κB and PPARγ were used to verify the role of NF-κB/ PPARγ/caspase 3 pathway in brucine-induced cytotoxicity and neurotoxicity in neuro-2a cells and primary astrocytes. The results showed that PPARγ inhibitor (GW9662) dramatically decreased cell viability and increased LDH level after brucine treatment; while, NF-κB inhibitor (Gliotoxin) and caspase 3 inhibitor (DEVE-FMK) significantly increased the cell viability and decreased LDH level after challenged by brucine (Figure 8A-D). These findings indicate that brucine-induced neurotoxicity, at least partly, through activation of NF-κB/PPARγ/caspase 3-dependent pathway.

Brucine directly bound to caspase 3

Molecular docking was utilized to further explore the interaction between brucine and caspase 3. The results showed that docking score of brucine with caspase 3 was -5.21 kcal/mol and the suppositive binding sites between brucine and caspase 3 including THR62, VAL-4, Gly122, and Cys163 (Figure 9). These findings confirm that caspase 3 might be the potential target of brucine-induced neurotoxicity.

Discussion

The present study, for the first time, revealed that: (1) Brucine-induced neurotoxicity, at least partly, through mediation of PPARγ/NF-κB/apoptosis signaling pathway. (2) Brucine-induced apoptosis due to it directly bound with caspase 3 and inhibited its activity (Fig. 10).

Emerging evidence demonstrates that brucine exerts anti-tumor, anti-inflammatory and analgesic effect in clinic. Albeit brucine has a striking pharmacological profile, severe neurotoxicity is the primary barrier to its clinical application (Lu et al. 2020; Zhou et al. 2019), and the toxicological mechanism of brucine was still unknown. The present study indicated that brucine significantly induced neurotoxicity as evidenced by determination of neuronal cell viability and LDH release, which is consistent with previous study (Shi et al. 2018; Gao et al. 2021). Notably, PPARs, NF-κB and apoptosis signaling pathway were predicted during brucine-induced cytotoxicity by transcriptome analysis. PPARs are the nuclear hormone receptors superfamily and can be categorized as three isoforms of PPAR-α, PPAR-β/δ and PPAR-γ, which plays vital roles in improving glucose and lipid homeostasis, inhibiting neuroinflammation and oxidative stress (Chistyakov et al. 2020; Zolezzi et al. 2017). Among them, PPARγ plays a crucial role in the mediation of inflammatory and immune reactions (Zuo et al. 2019; Gao et al. 2021). The activation of PPARγ adjusts the release of pro-inflammatory factors through mediating the transcription factors activity, such as NF-κB (Wang et al. 2017; Lee et al. 2018). Our findings indicated that brucine apparently inactivated the PPARγ, but did not affect the PPAR-α and PPAR-β/δ, then reduced pro-inflammatory factors release *via* promoting phosphorylation of NF-κB, in keeping with the predicted results of transcriptome analysis. Furthermore, we also utilized PPARγ inhibitor and NF-κB inhibitor to verify the role of PPARγ and NF-κB in brucine-induced neurotoxicity. As expected, PPARγ inhibitor aggravated the neurotoxicity, while, NF-κB inhibitor substantially reversed brucine-induced neurotoxicity. Interestingly, recent studies report that PPARs directly associated with apoptosis (Cheng et al. 2021; Thulasi Raman et al. 2020). The results showed that brucine significantly increased the pro-apoptosis protein Bax and decreased the anti-apoptosis protein Bcl-2, as well as elevated the level cleaved caspase 3 protein and its activity. Intriguingly, brucine directly bound to caspase 3, and caspase 3 inhibitor dramatically inhibited brucine-induced neurotoxicity. Our results showed that once PPARγ was suppressed, Bax increased and Bcl-2 decreased, which could evoke apoptosis; while, brucine inhibited PPARγ, thereby increased the ratio of Bax/Bcl-2 and activation of caspase 3. These findings indicate that brucine-induced neurotoxicity through mediating PPARγ/NF-κB/caspase 3 signaling pathway.

It should be noted that although low level concentrations of brucine were found in brain, it could induce metabolic acidosis and injure the brain due to its direct poisons or the influence on neurotransmitters in the central nervous system. Brucine has been proved to penetrate the blood brain barrier (BBB) in animal model (Ren et al. 2018; Li et al. 2018), however, there is still lack of reference data about the detailed clinical pharmacokinetic studies. What is more, this study preliminary reveals the neurotoxicity of brucine *in vitro*, the exact mechanism or target of brucine remains still a mystery. Thus, the detailed pharmacokinetics including evidence that brucine crosses BBB and the levels of brucine in brain tissue or cerebrospinal fluid in patients and the mechanism of brucine-induced neurotoxicity will be further elucidated utilized clinic trial or the animal models in our next story.

Conclusion

Collectively, our findings reveal that brucine-induced neurotoxicity by targeting caspase 3 through mediating PPARγ/NF-κB/apoptosis signaling pathway. Inhibition of caspase 3 and activation of PPARγ may be a promising therapeutic tactics for antagonizing brucine-induced neurotoxicity.

Declarations

Funding

This work was supported by Natural Science Foundation of China (No. 82060730), Post subsidy project of State key R & D plan in social development field (No. SQ2017YFC170204-05), Program for Changjiang Scholars and Innovative Research Team in University, China (RT_17R113), Science and Technology Support Plan of Guizhou Province (No. [2020]1Y010), Innovative Research Team of comprehensive utilization with *Lithocarpus polystachyus* Rehd sweet tea in Zunyi City (No. [2021]4).

Conflict of Interest The authors declare no competing interests.

Disclaimers The authors indicate that the views expressed in the submitted article are their own and not an official position of the institution or the funding agency**.**

References

1. Savalia R, Chatterjee S (2017) Sensitive detection of brucine an anti-metastatic drug for hepatocellular carcinoma at carbon nanotubes-nafion composite based biosensor. Biosens Bioelectron 98: 371-377
2. Ma JB, Qiu HW, Rui QH, Liao YF, Chen YM et al (2018) Enhanced cleanup efficiency hydroxy functionalized-magnetic graphene oxide and its comparison with magnetic carboxyl-graphene for PRiME pass-through cleanup of strychnine and brucine in human plasma samples. Anal Chim Acta 1020: 41-50

3. Li S, Chu Y, Zhang R, Sun L, Chen X (2018) Prophylactic neuroprotection of total glucosides of paeoniae radix alba against semen strychni-induced neurotoxicity in rats: suppressing oxidative stress and reducing the absorption of toxic components. Nutrients 10: 514
4. Gao L, Lin Y, Wang S, Lin L, Lu D et al (2021) Chronotoxicity of Semen Strychni is associated with circadian metabolism and transport in mice. J Pharm Pharmacol 73(3) 398-409
5. Liu F, Wang X, Han X, Tan X, Kang W (2015) Cytotoxicity and DNA interaction of brucine and strychnine-Two alkaloids of semen strychni. Int J Biol Macromol 77: 92-98
6. Seeman JI, Tantillo, DJ (2020) From decades to minutes: steps toward the structure of strychnine 1910-1948 and the application of today's technology. Angew Chem Int Ed Engl 59(27):10702-10721
7. Zheng L, Wang X, Luo W, Zhan Y, Zhang Y (2013) Brucine, an effective natural compound derived from nux-vomica, induces G1 phase arrest and apoptosis in LoVo cells. Food Chem Toxicol 58: 332-339
8. Dang J, Tiwari SK, Agrawal K, Hui H, Qin Y et al (2021) Glial cell diversity and methamphetamine-induced neuroinflammation in human cerebral organoids. Mol Psychiatry 26(4): 1194-1207
9. Pei X, Jiang H, Liu X, Li L, Li C et al (2021) Targeting HMGB1 inhibits T-2 toxin-induced neurotoxicity via regulation of oxidative stress, neuroinflammation and neuronal apoptosis. Food Chem Toxicol 151: 112134
10. Seshadri VD (2021). Brucine promotes apoptosis in cervical cancer cells (ME-180) via suppression of inflammation and cell proliferation by regulating PI3K/AKT/mTOR signaling pathway. Environ Toxicol 36(9): 1841-1847
11. Hong Y, Liu Q, Peng M, Bai M, Li J et al (2020) High-frequency repetitive transcranial magnetic stimulation improves functional recovery by inhibiting neurotoxic polarization of astrocytes in ischemic rats. J Neuroinflammation 17(1): 150
12. Ney GM, Yang KB, Ng V, Liu L, Zhao M et al (2021) Oncogenic N-Ras mitigates oxidative stress-induced apoptosis of hematopoietic stem cells. Cancer Res 81(5): 1240-1251
13. Wang Q, Zhu Q, Ye Q, Wang J, Dong Q et al (2020) STAT3 suppresses cardiomyocytes apoptosis in CVB3-induced myocarditis via survivin. Front Pharmacol 11: 613883
14. Reyna DE, Garner TP, Lopez A, Kopp F, Choudhary GS et al (2017) Direct activation of BAX by BTSA1 overcomes apoptosis resistance in acute myeloid leukemia. Cancer Cell 32(4): 490-505 e410
15. Yang X, Xiao Y, Zhong C, Shu F, Xiao S et al (2020) ABT-263 reduces hypertrophic scars by targeting apoptosis of myofibroblasts. Front Pharmacol 11: 615505
16. Chung Y, Lee J, Jung S, Lee Y, Cho JW et al (2018) Dysregulated autophagy contributes to caspase-dependent neuronal apoptosis. Cell Death Dis 9(12): 1189
17. Huang R, Xu Y, Lu X, Tang X, Lin J et al (2021) Melatonin protects inner retinal neurons of newborn mice after hypoxia-ischemia. J Pineal Res 71(1): e12716
18. Bahrami A, Amerizadeh F, ShahidSales S, Khazaei M, Ghayour-Mobarhan M et al (2017) Therapeutic potential of targeting Wnt/β-catenin pathway in treatment of colorectal cancer: rational and

progress. J Cell Biochem 118(8): 1979-1983

19. Zheng Y, Deng Y, Gao JM, Lv C, Lang LH et al (2020) Icariside II inhibits lipopolysaccharide-induced inflammation and amyloid production in rat astrocytes by regulating IKK/I-κB/NF-κ/BACE1 signaling pathway. Acta Pharmacol Sin 41 (2): 154-162
20. Lu L, Huang R, Wu Y, Jin JM, Chen HZ et al (2020) Brucine: A review of phytochemistry, pharmacology, and toxicology. Front Pharmacol 11: 377
21. Zhou Z, Lin Y, Gao L, Yang Z, Wang S et al (2019) Cyp3a11 metabolism-based chronotoxicity of brucine in mice. Toxicol Lett 313: 188-195
22. Shi X, Zhu M, Kang Y, Yang T, Chen X et al (2018) Wnt/beta-catenin signaling pathway is involved in regulating the migration by an effective natural compound brucine in LoVo cells. Phytomedicine 46: 85-92
23. Gao L, Lin Y, Wang S, Lin L, Lu D et al (2021) Chronotoxicity of Semen Strychni is associated with circadian metabolism and transport in mice. J pharm pharmacol 73(3): 398-409
24. Chistyakov DV, Astakhova AA, Goriainov SV, Sergeeva MG (2020) Comparison of PPAR ligands as modulators of resolution inflammation, via their influence on cytokines and oxylipins release in astrocytes. Int J Mol Sci 21(24): 9577
25. Zolezzi JM, Santos MJ, Bastias-Candia S, Pinto C, Godoy JA et al (2017) PPARs in the central nervous system: roles in neurodegeneration and neuroinflammation. Biol Rev Camb Philos Soc 92(4): 2046-2069
26. Zuo Y, Huang L, Enkhjargal B, Xu W, Umut O et al (2019) Activation of retinoid X receptor by bexarotene attenuates neuroinflammation via PPARγ/SIRT6/FoxO3a pathway after subarachnoid hemorrhage in rats. J Neuroinflammation 16(1): 47
27. Gao Z, Xu X, Li Y, Sun K, Yang M et al (2021) Mechanistic insight into PPARγ and tregs in atherosclerotic immune inflammation. Front Pharmacol 12: 750078
28. Wang K, Li YF, Lv Q, Li XM, Dai Y et al (2017) Bergenin, acting as an agonist of PPARγ, ameliorates experimental colitis in mice through improving expression of SIRT1, and therefore inhibiting NF-κB-mediated macrophage activation. Front Pharmacol 8: 981
29. Lee EJ, Park JS, Lee YY, Kim DY, Kang JL et al (2018) Anti-inflammatory and anti-oxidant mechanisms of an MMP-8 inhibitor in lipoteichoic acid-stimulated rat primary astrocytes: involvement of NF-κB, Nrf2, and PPAR-γ signaling pathways. J neuroinflammation 15(1): 326
30. Cheng Z, Guo C (2021) Pemafibrate pretreatment attenuates apoptosis and autophagy during hepatic ischemia-reperfusion injury by modulating JAK2/STAT3/PPAR pathway. PPAR Res 2021: 6632137
31. Thulasi Raman SN, Latreille E, Gao J, Zhang W, Wu J et al (2020) Dysregulation of Ephrin receptor and PPAR signaling pathways in neural progenitor cells infected by Zika virus. Emerg Microbes Infect 9(1): 2046-2060
32. Ren T, Li M, Zheng H, Liu W, Zhang J (2018) Microdialysis combined with RRLC-MS/MS for the pharmacokinetics of two major alkaloids of Bi qi capsule and the potential roles of P-gp and BCRP

on their penetration. J Chromatogr B Analyt Technol Biomed Life Sci 1092: 72-81

Figures

Figure 1

Brucine induced cytotoxicity in Neuro-2a cells. (A) Chemical structure of brucine. Neuro-2a cells were treated with brucine at different concentrations (1, 4 and 16 μM) for 24 h. (B) Cell viability was detected using MTT assay (n= 5). (C) LDH release from Neuro-2a cells was measured using commercial LDH assay kit (n= 5). (D) Neuro-2a cells was observed by phase contrast microscopy (200 ×, Scale bar=50 μm). The data were presented as the mean ± SD. $^{*}P<0.05$, $^{**}P<0.01$ *vs* control group.

Figure 2

Transcriptome analysis. (A) Analysis of PCA between control and brucine groups (n= 5). (B) Volcano plot (n= 5). (C) Hierarchical clustering (n= 5). (D) Analysis of KEGG pathway (n= 5).

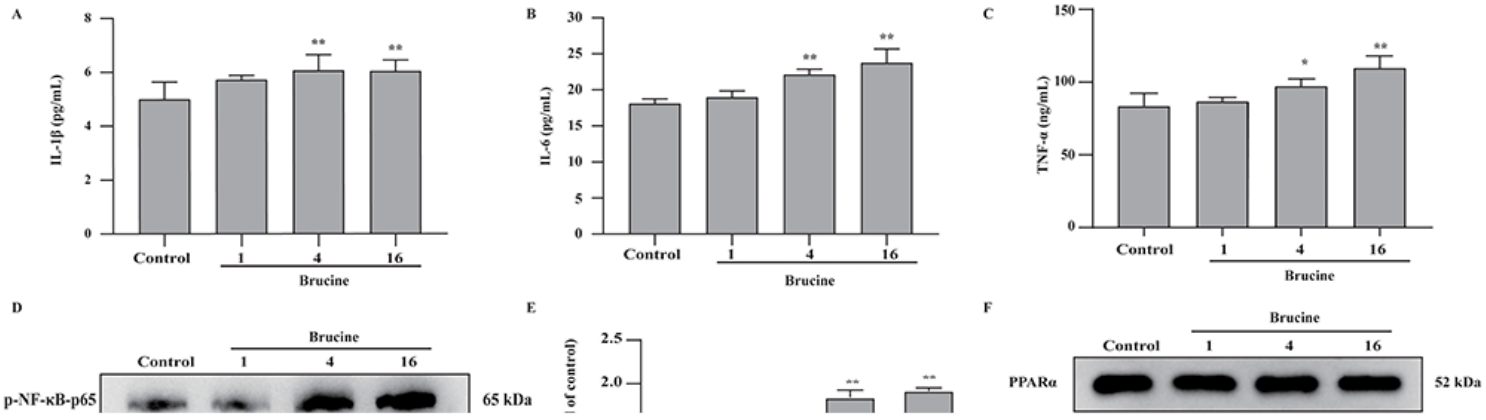

Figure 3

Brucine elicited inflammatory cytokines through regulating PPARγ/NF-κB pathway. (A) IL-1β level (n=5). (B) IL-6 level (n=5). (C) TNF-α level (n=5). (D) Representative Western blot of phosphorylation level of NF-κBp65. (E) Quantitation of phosphorylation level of NF-κBp65 (n=3). (F) Representative Western blot of PPARα, PPAR-β/δ and PPARγ protein expressions. (G) Quantitation of PPARα protein expression (n=3). (H) Quantitation of PPAR-β/δ protein expression (n=3). (I) Quantitation of PPARγ protein expression (n=3). The data were presented as the mean ± SD. $^{*}P<0.05$, $^{**}P<0.01$ *vs* control group.

Figure 4

Brucine induced apoptosis in Neuro-2a cells. Neuro-2a cells exposed to brucine (1, 4, 16 μM) for 24 h. (A) Representative images of TUNEL staining in the Neuro-2a. (B) Quantitative analysis of TUNEL-positive cells in the Neuro-2a (n=3). (C) Apoptosis was analyzed using flow cytometry. (200 ×, Scale bar=50 μm). The data were presented as the mean ± SD. $^{*}P<0.05$ *vs* control group.

Figure 5

Brucine induced apoptosis by activation of caspase 3 pathway in Neuro-2a cells. Neuro-2a cells were exposed to brucine (1, 4, 16 μM) for 24 h. (A) Representative western blot of Bax, Bcl-2, cleaved-caspase 3 and caspase 3. (B) Quantitation of Bax/Bcl-2 ratio (n = 5). (C) Quantitation of cleaved-caspase-3/caspase-3 (n = 5). (D) Caspase-3 activity (n = 5).The data were presented as the mean ± SD. $^{**}P<0.01$ *vs* control group.

Figure 6

Brucine induced neurotoxicity on primary astrocytes. Primary astrocytes were treated with brucine at different concentrations (8, 16 and 32 μM) for 24 h. (A) Cell viability was determined using MTT assay (n = 5) (B) LDH release from primary astrocytes was measured using commercial LDH assay kit (n = 5). (C) The morphology of primary astrocytes were observed after brucine treatment. (200 ×, Scale bar=200 μm). The data were presented as the mean ± SD. $^{*}P<0.05$, $^{**}P<0.01$ *vs* control group.

Figure 7

Brucine promoted the release of inflammatory factors in primary astrocytes. Primary astrocytes were exposed to brucine (8, 16, 32 μM) for 24 h. (A) IL-1β level (n=5). (B) IL-6 level (n=5). (C) TNF-α level (n=5). (D) Representative Western blot of phosphorylation level of NF-κBp65. (E) Quantitation of phosphorylation of NF-κBp65 protein level (n = 3). (F) NF-κBp65 binding activity (n=5). (G) Representative Western blot of PPARγ protein expression. (H) Quantitation of PPARγ protein expression (n = 3). (I) DNA binging activity of PPARγ (n=5). (J) Representative western blot of Bax and Bcl-2 protein expressions. (K) Quantitation of Bax/Bcl-2 ratio (n = 3). (L) Caspase-3 activity (n=5). The data were presented as the mean ± SD. $^{*}P<0.05$, $^{**}P<0.01$ *vs* control group.

Figure 8

Brucine induced neurotoxicity via mediating NF-κB/PPARγ/caspase 3 signaling pathway. Neuro-2a cells were treated with brucine at different concentrations (1, 4, or 16 μM) for 24 h and with or without DEVE-

FMK, GW 9662 or Gliotoxin. (A) Cell viability was determined using MTT assay. (B) LDH level. Primary astrocytes were treated with brucine at different concentrations (8, 16, or 32 μM) for 24 h and with or without DEVE-FMK, GW 9662 or Gliotoxin. (C) Cell viability. (D) LDH release. The data were presented as the mean ± SD. $^{*}P<0.05$, $^{**}P<0.01$ *vs* control group; $^{\#\#}P<0.01$, $^{\$\$}P<0.01$, $^{\&\&}P<0.01$ *vs* brucine 16 or brucine 32 group.

Figure 9

Brucine directly bound with caspase 3. (A) Amino acid residues. (B) A visual of the binding sites between brucine and caspase 3. (C) The substrate binding pocket.

Figure 10

Presentation of a proposed mechanism for brucine-induced neurotoxicity. Brucine not only directly binds to caspase 3 and increases its activity, but also mediates PPARγ/NF-κB/apoptosis signaling pathway, thereby promoting inflammatory cytokines.

Supplementary Files

This is a list of supplementary files associated with this preprint. Click to download.

- Originalwesternblots.pdf